# Coupling of intramolecular and intermolecular linkage complexity of two DNAs

John F. Marko
*Department of Physics, The University of Illinois at Chicago, 845 West Taylor Street, Chicago, Illinois 60607*
(Received 29 April 1998)

The free energy of two interlinked circular DNAs is argued to couple their interlinkage (catenation) to their ''internal'' double-helix linkages. Changes in internal linkage which drive supercoiling can therefore alter the free-energy cost of intermolecule catenations. This effect is weak for low amounts of supercoiling or catenation, but becomes strong when there is more than one link added per persistence length. DNA supercoiling can therefore increase the free-energy cost of interlinkages, and in living cells can help to direct type-II topoisomerases to remove catenations between DNAs following their replication, a process required for the segregation of the duplicate molecules. The related problem of the interaction of applied tension with catenation and supercoiling is also analyzed. [S1063-651X(98)10512-3]

PACS number(s): 87.15.−v, 36.20.Ey, 64.90.+b

## I. INTRODUCTION

The free-energy cost of constraint of fluctuations of flexible polymers is an essential ingredient of polymer physics. Some constraints of interest are geometrical, an important example being constraint of the distance between the ends of a random-coil polymer which reduces the number of configurations of the chain, decreasing conformational entropy and increasing free energy [1]. The result is that work must be done to stretch a flexible polymer: flexible polymers exhibit entropic elasticity.

A second class of constraints relevant to the circular double-helix DNAs of bacterial cells are topological [2,3]. Perhaps the simplest topological property of a single circular DNA is the linkage number Lk of its two nucleotide strands, the number of times one strand winds around the other. Lk is an integer-valued topological invariant, staying constant as long as the two strands remain unbroken. This ''internal'' linkage number of the double helix is of biological importance: bacterial cells enzymatically control the internal linkage of their circular ''plasmid'' and chromosomal DNAs [4].

To understand the free-energy cost of constraint of Lk one must understand how linkage is partitioned between DNA twist, and chiral bending or ''writhing'' of the backbone. For sufficient perturbation of Lk, a DNA will respond by ''supercoiling'' or wrapping around itself in the manner of a twisted telephone cord. This wrapping occurs roughly when $1/2\pi$ of a link has been added or removed per thermal twisting persistence length (roughly 100 nm or 300 base pairs or bp); at this point the entropy lost by bringing the molecule close to itself to form the supercoil is comparable to the twist energy saved [5]. The statistical mechanics of supercoiled DNAs has been illuminated via experimental studies of free energies [6], conformations [7,8], and elasticity [9,10]. Corresponding theoretical work has proceeded along both simulation [2,11,12] and analytical [5,13–15] lines.

Given two DNAs, a second type of topological constraint analogous to Lk can be considered, the interlinkage of the two double helices. When the two double helices form a simple toroidal braid (Fig. 1), this can be quantified with an integer, the catenation number Ca. Catenated DNAs have also been studied via analytical and computer simulation approaches; the increase in the free energy of the chains with Ca and some of their elastic properties have been predicted [16]. Experiments on catenated chains have included studies of thermodynamical equilibrium of topology [17,18], conformation using electron microscopy [19], and elasticity using micromanipulation [10]. Catenanes are of interest to biologists because toroidal catenanes are intermediates in the process of DNA replication in bacterial cells [20,21]; of course all catenations must be removed between the two identical DNAs produced by DNA replication in order for them to be segregated [22].

This paper discusses the free energy of two entangled

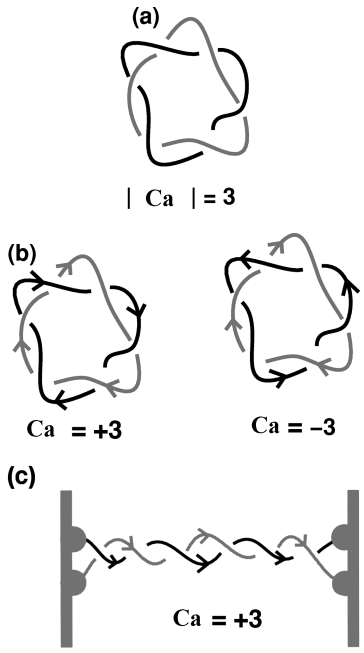


FIG. 1. (a) Two toroidally catenated plasmids with right-handed interwinding and $|\mathrm{Ca}|=3$; (b) the Gauss linking number for (a) is $\pm 3$, depending on how the chains are directed; (c) anchoring the chains on two parallel walls which are free to translate in $z$ defines chain directedness, and eliminates translational entropy from the problem. For toroidal catenation the Gauss linking number represents the number of times one wall is twisted with respect to the other.

 

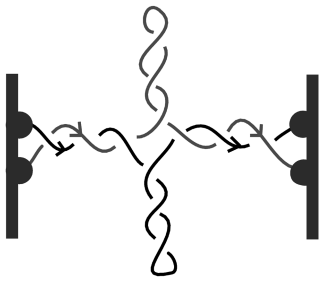


FIG. 2. If toroidally catenated DNAs are supercoiled, formation of plectonemic supercoil domains ''crowds'' the catenations. This effect leads to a coupling of catenation and double-helix linkage for more than one link of either type per persistence length.

double-helix DNAs, subject to the additional intramolecular constraint of their internal linkage numbers. The main result is that the free energy couples Lk to Ca. However, for small amounts of supercoiling and catenation where the chains are only slightly perturbed from random walks, the coupling of catenation to internal double-helix linkage is very weak (Sec. II A). By contrast, for large amounts of supercoiling or catenation (more than one link of either type added per thermal persistence length), the chains become tightly coiled, and the coupling of supercoiling to catenation becomes strong (Sec. II B). This comes about via ''crowding'' of the catenations by the plectonemic supercoiling driven by Lk (Fig. 2). Effects of this coupling have already been observed in simulations of topological equilibrium of supercoiled DNAs, in the form of a strong suppression of the catenation probability of supercoiled DNAs [18].

Effects of catenation-supercoiling coupling on the elasticity of braided and supercoiled DNAs are discussed in Sec. III, by considering the two DNAs to be individually subject to twisting torques, and also to a mutual torque which interwinds the two chains. In the high-force limit, a method similar to that of Moroz and Nelson [13] and Bouchitat and Mezard [14] shows that the elasticity of the resulting braid of supercoils couples the intramolecular torque to the intermolecular torque. These effects could be studied experimentally in micromanipulation experiments.

Finally, in the summary (Sec. IV) the relevance of the paper to the biophysical problem of segregation of toroidally catenated DNAs is discussed. For a ''parent'' DNA to be replicated and the resultant copies segregated, its two strands must be unwound [22]. Because of the inevitable failure to remove all of these interwinds, replicated DNAs are toroidally catenated before the action of a decatenating enzyme, topoisomerase (topo) IV. Efficient operation of this enzyme in the cell requires DNA supercoiling [23–25]. This observation can be understood via the results of Sec. II, which indicate that supercoiling can provide a strong thermodynamic driving force for catenation removal.

## II. FREE ENERGY OF CATENATED, SUPERCOILED DNAS

Consider two circular DNAs of length $L$, each with a double-helix excess linkage $\Delta\mathrm{Lk}$. The excess linkage is relative to the linkage of relaxed DNA, $\mathrm{Lk}_0 = L/h$, where $h$ is the helix repeat $\approx 3.5$ nm or 10.5 base pairs (bp). The plasmid conformations are described by two curves $\mathbf{r}_i(s)$, $i=1,2$. For the purposes of this paper DNA may be regarded as inextensible (for a discussion of DNA elasticity for high forces, see [26]), and so arc length $s$ corresponds to genomic distance along the molecules (1 nm $\approx 3$ bp), and the tangents $\hat{\mathbf{t}}_i = d\mathbf{r}_i/ds$ are unit vectors. The energy is

$$\frac{E}{k_B T} = \sum_i^{1,2} \int_0^L ds \left\{ \frac{A}{2} \left( \frac{d\hat{\mathbf{t}}_i}{ds} \right)^2 + 2\pi C (\Delta \mathrm{Tw}_i)^2 \right\} + \text{hard core interactions} \tag{1}$$

where the bending persistence length $A \approx 50$ nm and the twisting persistence length $C \approx 75$ nm [27] (the precise values of these constants, the addition of other elastic terms to the free energy, and the straightforward generalization to differing lengths or duplex linkages for the two plasmids are all unimportant to the aim of this paper). The hard-core interactions are short-ranged, and for ''physiological'' aqueous solution (e.g., pH 7.4 PBS with 0.15 M NaCl) can be thought of as simply keeping regions of double helix from coming closer than $\approx 3$ nm to one another.

The twist energy depends on the total excess twist which in turn depends on linkage through the relation $\Delta\mathrm{Tw}_i = \Delta\mathrm{Lk} - \mathrm{Wr}_i$, where the ''writhes'' $\mathrm{Wr}_i$ account for the contribution of nonlocal crossovers of the molecules to linkage [28]:

$$\mathrm{Wr}_i = \frac{1}{4\pi} \int ds \int ds' \hat{\mathbf{t}}_i(s) \times \hat{\mathbf{t}}_i(s') \cdot \frac{\mathbf{r}_i(s) - \mathbf{r}_i(s')}{|\mathbf{r}_i(s) - \mathbf{r}_i(s')|^3}. \tag{2}$$

This basic model quantitatively describes many aspects of supercoiled and decatenated plasmids [5,7].

Thermal fluctuations of Eq. (1) will be considered subject to the additional constraint of fixed Gaussian mutual linkage number Ca, which for directed chains is

$$\mathrm{Ca} = \frac{1}{4\pi} \int_0^L ds \int_0^L ds' \hat{\mathbf{t}}_1(s) \times \hat{\mathbf{t}}_2(s') \cdot \frac{\mathbf{r}_1(s) - \mathbf{r}_2(s')}{|\mathbf{r}_1(s) - \mathbf{r}_2(s')|^3}. \tag{3}$$

For toroidal catenation of unknotted plasmids (e.g., Fig. 1), Ca is simply the signed number of wrappings of one DNA around the other. The combination of constraint of Eq. (3) and the energy (1) with twists replaced by linkages and writhes is the basic model of interest here.

The same basic model with slightly different boundary conditions describes the situation where the two molecules are each suspended between impenetrable walls [Fig. 1(c)] which are perpendicular to, and able to freely translate along, a given direction (the $z$ axis). For simple toroidal interlinkage of the two DNAs, Eq. (3) represents the signed wrapping of one chain around the other introduced by twisting one wall around the $z$ axis as might be done in a micromanipulation experiment. Most of the analysis of this paper will be done with the boundary conditions of Fig. 1(c) in mind; also note that the limit of long chains ($L \gg A$) is assumed.

If excluded-volume interactions are included to keep the chains from intersecting, then the free energy $F(\Delta\mathrm{Lk},\mathrm{Ca})$

follows from summation of the Boltzmann weights for all permitted configurations. In this paper the free energy is estimated as a function of Ca and ΔLk. Detailed numerical results from simulations of this model will be reported elsewhere [29].

### A. Small amounts of linkage and toroidal catenation

For large $L$ and small ΔLk and Ca (''how small'' will be clarified below) one expects an expansion for the free energy of each chain relative to that for ΔLk=Ca=0,

$$\frac{F}{k_BT}=\frac{a}{2}\Delta\mathrm{Lk}^2+\frac{b}{2}\mathrm{Ca}^2+c\,\Delta\mathrm{Lk}\,\mathrm{Ca}+\text{quartic terms}. \quad (4)$$

There is no linear ΔLk term because the state ΔLk=0 is by assumption the minimum free-energy state for Ca=0. The linear Ca and higher-odd-order terms are absent because space inversion is a symmetry of the energy (1), and reverses the signs of ΔLk or Ca *together* (since the DNA double helix is itself chiral, this symmetry may be weakly broken, e.g., by couplings of twist to bend [30]).

For the boundary conditions of Fig. 1(c), there is no symmetry of the energy which reverses only one of ΔLk and Ca, since such a transformation would change the handedness of the individual plasmid conformations without a change in handedness of their mutual entanglement. For these boundary conditions it is plausible that Eq. (4) couples the two topological charges, or $c\neq 0$. The sign of $c$ can be argued to be negative by considering Fig. 1(c). For toroidal catenanes with Ca>0, the right-handed wrapping of one chain around the other induces Wr>0. Twist energy and therefore free energy should be reduced when ΔLk>0, or $c<0$.

The coupling $c$ can be further understood by considering an ensemble where ΔLk and Ca freely fluctuate, or where the chains are ''phantom polymers'' with no barriers to their crossings. Then the equilibrium distribution of topoisomers is just $\exp[-F(\Delta\mathrm{Lk},\mathrm{Ca})/k_BT]$ [for free circular DNAs one should take care to properly account for the translational entropy of the completely unlinked Ca=0 state; this is unnecessary for the anchored chains of Fig. 1(c) as long as the anchor points are not permitted to wander far apart in the *x*-*y* plane]. For the phantom chain ensemble, the constant $c$ indicates the tendency for writhe fluctuations to induce linkage, or vice versa. Consider a fluctuation with positive writhe of one chain: there will be some right-handed coils in that chain, which will tend to make positive links with even a chirally unbiased second chain. This indicates that for phantom chains and the geometry of Fig. 1(c), $\langle\Delta\mathrm{LkCa}\rangle>0$, and again indicates that $c$ in the fixed-topology ensemble should be negative.

The next question is how the coefficients $a$, $b$, and $c$ scale with persistence length and molecule length. It is again convenient to consider spontaneous fluctuations of ΔLk and Ca in a phantom chain ensemble, and to compute the correlations $\langle\Delta\mathrm{Lk}^2\rangle$, $\langle\mathrm{Ca}^2\rangle$, and $\langle\Delta\mathrm{Lk}\,\mathrm{Ca}\rangle$. The free energy which generates these expectation values may then be obtained. These correlations can be estimated for the purely random-coil fluctuations of the fluctuating-topology phantom ensemble using a power-counting scheme [5,15] (coil swelling due to self-avoidance is ignored here, which is reasonable for DNAs of <100 kb; the ratio of exclusion diameter to Kuhn length, $d/2A=0.03$, determines this limit [5]).

In the phantom random coil ensemble, twisting and bending fluctuations are independent, so $\langle\Delta\mathrm{TwWr}\rangle=0$, and $\langle\Delta\mathrm{Lk}^2\rangle=\langle\Delta\mathrm{Tw}^2\rangle+\langle\mathrm{Wr}^2\rangle$. The free twist fluctuations of Eq. (1) give $\langle\Delta\mathrm{Tw}^2\rangle=L/(4\pi C)$. The writhe fluctuations are

$$\langle\mathrm{Wr}^2\rangle=\frac{1}{16\pi^2}\int ds\int ds'\int ds''\int ds'''\left\langle\left(\hat{\mathbf{t}}(s)\times\hat{\mathbf{t}}(s')\cdot\frac{\mathbf{r}(s)-\mathbf{r}(s')}{|\mathbf{r}(s)-\mathbf{r}(s')|^3}\right)\left(\hat{\mathbf{t}}(s'')\times\hat{\mathbf{t}}(s''')\cdot\frac{\mathbf{r}(s'')-\mathbf{r}(s''')}{|\mathbf{r}(s'')-\mathbf{r}(s''')|^3}\right)\right\rangle. \quad (5)$$

Since the orientational correlation along the chains falls off with range $A$, $\langle\hat{\mathbf{t}}(s)\cdot\hat{\mathbf{t}}(s')\rangle=e^{|s-s'|/A}$, the only contribution to Eq. (5) comes when $|s-s''|<A$ and $|s'-s'''|<A$, or when $|s-s'''|<A$ and $|s'-s''|<A$. Keeping only these ranges in the integral and estimating the denominators using the random walk result $\langle|\mathbf{r}(s)-\mathbf{r}(s')|^2\rangle=2A|s-s'|$ gives

$$\langle\mathrm{Wr}^2\rangle\approx\int_0^L ds\int_0^L ds'\frac{1}{(|s-s'|^2+A^2)}\approx L/A. \quad (6)$$

The cutoff of the singularity in the denominator puts the correct $\mathcal{O}(1)$ bound on the writhe contribution of nearby statistical segments (the statistical segment length or Kuhn length is $2A$).

The same approach leads to an estimate for $\langle\mathrm{Ca}^2\rangle$,

$$\langle\mathrm{Ca}^2\rangle=\frac{1}{16\pi^2}\int ds\int ds'\int ds''\int ds'''\times\left\langle\left(\hat{\mathbf{t}}_1(s)\times\hat{\mathbf{t}}_2(s')\cdot\frac{\mathbf{r}_1(s)-\mathbf{r}_2(s')}{|\mathbf{r}_1(s)-\mathbf{r}_2(s')|^3}\right)\left(\hat{\mathbf{t}}_1(s'')\times\hat{\mathbf{t}}_2(s''')\cdot\frac{\mathbf{r}_1(s'')-\mathbf{r}_2(s''')}{|\mathbf{r}_1(s'')-\mathbf{r}_2(s''')|^3}\right)\right\rangle \quad (7)$$

for two random walks, subject to the caveat that they set out from nearby staring points [e.g., the anchors introduced in Fig. 1(c)]. So, in addition to random walk statistics along each contour, there are also random walk statistics governing the separation of the two chains, $\langle|\mathbf{r}_1(s)-\mathbf{r}_2(s')|\rangle=2A|s+s'|$, where here their mutual starting point is taken to be at $s=s'=0$. Only the regions $|s-s''|<A$ and $|s'-s'''|<A$ contribute to the integral, giving

$$\langle \mathrm{Ca}^2 \rangle \approx \int_0^L ds \int_0^L ds' \frac{1}{(|s+s'|^2+A^2)} \approx \ln \frac{L}{A}. \tag{8}$$

The distribution for catenation is much narrower than for writhe, because the *two* random walks involved in Eq. (7) tend to wander away from one another, making successive wrappings occur at progressively greater intervals in contour length. The scaling of Eq. (8) was previously obtained for flexible polymer models [31,32].

Finally, one can estimate the correlation of link and catenation, again using the independence of twist and bending fluctuations to reduce $\langle \Delta \mathrm{LkCa} \rangle = \langle \mathrm{CaWr} \rangle$,

$$\langle \Delta \mathrm{LkCa} \rangle = \frac{1}{16\pi^2} \int ds \int ds' \int ds'' \int ds''' \left\langle \left( \hat{\mathbf{t}}_1(s) \times \hat{\mathbf{t}}_1(s') \cdot \frac{\mathbf{r}_1(s) - \mathbf{r}_1(s')}{|\mathbf{r}_1(s) - \mathbf{r}_1(s')|^3} \right) \left( \hat{\mathbf{t}}_1(s'') \times \hat{\mathbf{t}}_2(s''') \cdot \frac{\mathbf{r}_1(s'') - \mathbf{r}_2(s''')}{|\mathbf{r}_1(s'') - \mathbf{r}_2(s''')|^3} \right) \right\rangle. \tag{9}$$

For the boundary conditions of Fig. 1(c), the two chains walk away from nearby starting ($s=0$) points in initially correlated directions [Fig. 1(c)]. This direction correlation gives rise to a contribution to Eq. (9) when $|s'|<A$ and $|s'''|<A$ and $|s-s''|<A$. Thus Eq. (9) scales as

$$\langle \Delta \mathrm{LkCa} \rangle \approx A \int_0^L \frac{ds}{s^2+A^2} \approx +1. \tag{10}$$

The correlation (10) is positive. Its $\mathcal{O}(1)$ size indicates that it is dependent on the boundary condition chosen; the integral (10) is dominated by contributions from near to the anchor points, even though the effective interaction is long-ranged ($1/s^2$).

The required correlations are therefore

$$\langle \Delta \mathrm{Lk}^2 \rangle = \alpha \frac{L}{A}, \quad \langle \mathrm{Ca}^2 \rangle = \beta \ln \frac{L}{A}, \quad \langle \Delta \mathrm{Lk\,Ca} \rangle = \gamma, \tag{11}$$

where $\alpha$, $\beta$ and $\gamma$ are $\mathcal{O}(1)$ constants which could be easily determined from simulation of the wormlike chain. The constants $a$, $b$, and $c$ corresponding to the correlations (11) follow as

$$a = \frac{1}{\alpha L/A}, \quad b = \frac{1}{\beta \ln(L/A)}, \quad c = -\frac{\gamma}{\alpha\beta} \frac{1}{L/A \ln(L/A)}. \tag{12}$$

The coupling between ΔLk and Ca is very weak in the fluctuation (weak linkage) regime [$|\Delta \mathrm{Lk}| \gg L/A$ and $|\mathrm{Ca}| \gg (\ln L/A)^{1/2}$].

There are qualitative differences between the three results of Eq. (11). First, $\langle (\Delta \mathrm{Lk})^2 \rangle \sim L$, since writhe and twist fluctuations are correlated essentially only within the thermal persistence lengths for bending and twisting, respectively. On the other hand, $\langle (\mathrm{Ca})^2 \rangle \sim \ln L$. This much slower growth reflects the fact that as the two molecules random-walk apart from one another the correlation length for their intertwining fluctuations also grows. Still, catenation-squared diverges with $L$, and is determined by bending fluctuations along the entire length of the two chains. By comparison, the correlation between excess linkage and catenation (or that of writhing and catenation) is extremely weak; thermal fluctuations of ΔLk and Ca are nearly independent. The only appreciable contribution to $\langle \Delta \mathrm{LkCa} \rangle$ comes from near to the chain anchor points, and is therefore dependent on details of the chain boundary conditions.

### B. Tight supercoiling and toroidal catenation

When the total added internal and mutual linkages exceeds more than one per persistence length, the DNAs will not undergo appreciable random bending between double-helix crossings. In this regime, their free energy can be estimated by considering the competition between twist and bending energy (which tend to drive tight and well-ordered supercoil and catenane turns), and the entropy cost of forming such structures. Previously this kind of description was provided for both supercoils [5] and braided DNAs [16]. As in those previous works, the calculations of this section are mean-field and semiquantitative.

Given catenation Ca and duplex linkages ΔLk, linkage densities $\sigma = \Delta \mathrm{Lk}/\mathrm{Lk}_0$ and $\sigma_c = \mathrm{Ca}/\mathrm{Lk}_0$ can be defined. The two braided and supercoiled chains will be supposed to form distinct toroidal braid and plectonemic supercoil domains (Fig. 2). A fraction $x$ of each chain's contour is taken to form the plectonemic domain, leaving a fraction $1-x$ to form the toroidal braid. The supercoil pitch and radius are $P$ and $R$, and the toroidal braid pitch and radius $P_c$ and $R_c$ (the helix repeats are $2\pi P$ and $2\pi P_c$, respectively). It will be convenient to define $l = (R^2+P^2)^{1/2}$ and $l_c = (R_c^2+P_c^2)^{1/2}$, which are the lengths of chain in a radian of supercoil and braid, respectively. Finally, helix opening angles are defined via $\sin\theta = P/l$ and $\sin\theta_c = P_c/l_c$ [5].

The catenation of the two chains comes purely from the braid domain, and is $\mathrm{Ca} = \pm(1-x)L/(2\pi l_c)$ (in this section upper and lower signs correspond to right- and left-handed superhelicities, respectively). Given that $\mathrm{Lk}_0 = L/h$ and defining $\omega_0 = 2\pi/h$, the catenation density is just $\sigma_c = \pm(1-x)/(\omega_0 l_c)$. Therefore,

$$l_c = \frac{1-x}{\omega_0 |\sigma_c|}. \tag{13}$$

By contrast, the internal double-helix linkage density is made up of contributions from both the supercoil and braid domains, $\sigma = x\sigma_{\mathrm{sc}} + (1-x)\sigma_{\mathrm{br}}$ (Ref. [16] explains why this additive form is reasonable). The writhe densities for the supercoiled and braid domains follow from standard formulas for writhes of plectonemic and solenoidal supercoils [5],

$$w_{sc}=\frac{2\pi \mathrm{Wr}_{sc}}{L}=\mp\frac{\sin\theta}{l},$$
$$w_{br}=\frac{2\pi \mathrm{Wr}_{br}}{L}=\pm\frac{1-\sin\theta_c}{l_c}=\frac{1-\sin\theta_c}{1-x}\omega_0\sigma_c. \tag{14}$$

Now an estimate of the free energy of the structure of Fig. 2 can be made by adding together the bending energy, twist energy, and the entropy loss incurred by confining the DNA into the supercoiled and catenated domains. Per unit length of DNA, the free energy is

$$\frac{F}{2k_BTL}=x\left[\frac{A}{2}\frac{R^2}{l^4}+\frac{C}{2}(\omega_0\sigma_{sc}-\omega_{sc})^2+\frac{1}{(AR^2)^{1/3}}+v(R)\right]+(1-x)\left[\frac{A}{2}\frac{R_c^2}{l_c^4}+\frac{C}{2}(\omega_0\sigma_{br}-\omega_{br})^2+\frac{1}{(AR_c^2)^{1/3}}+v(R_c)\right]. \tag{15}$$

Hard-core potentials $v$ are included to keep the DNAs from coming closer than $\approx 3$ nm (the precise form of $v$ used is that of Refs. [5,16] for aqueous buffer with $\approx 0.15$ M univalent salt). The free energy (15) is a function of the undetermined parameters $x$, $l$, $R$, $\sigma_{sc}$, and $R_c$, which must be set by minimization [$l_c=(1-x)/(\omega_0|\sigma_c|)$ and $\sigma_{br}=(\sigma-x\sigma_{sc})/(1-x)$ are determined by these parameters]. This model is reasonable only when the length of molecule in a radian of either interwind is less than the bending persistence length, or when both $l<A$ and $l_c<A$ hold. Since the free energy arises from a balance between fluctuations and DNA elasticity, this is equivalent to requiring that the free energy per length be at least $k_BT/A \approx 0.02k_BT$/nm above that of an unperturbed random coil.

Minimization of the twist energies of Eq. (15) with respect to $\sigma_{sc}$ can be done analytically. The minimum occurs for equal DNA twisting torques in the two domains, or for

$$\omega_0\sigma_{sc}-\omega_{sc}=\omega_0\sigma_{br}-\omega_{br}=\omega_0\sigma-x\omega_{sc}-(1-x)\omega_{br}. \tag{16}$$

After plugging this into Eq. (15) the free energy becomes

$$\frac{F}{2k_BTL}=x\left[\frac{A}{2}\frac{\cos^2\theta}{l^2}+\left(\frac{1}{Al^2\cos^2\theta}\right)^{1/3}+v(l\cos\theta)\right]$$
$$+(1-x)\left[\frac{A}{2}\frac{\cos^2\theta_c}{l_c^2}+\left(\frac{1}{Al_c^2\cos^2\theta_c}\right)^{1/3}+v(l_c\cos\theta_c)\right]+\frac{C}{2}\left[\omega_0\sigma\pm\frac{x\sin\theta}{l}-(1-\sin\theta_c)\omega_o\sigma_c\right]^2. \tag{17}$$

The first two lines consist of the bending energy, entropy loss, and hard-core interactions. The last line is the DNA twisting energy, which contains writhe contributions from the supercoiled and catenated domains. In Eq. (17), $\theta$ and $\theta_c$ are taken to be between 0 and $\pi/2$; the chirality of the coils is set by the $\pm$ for the plectoneme writhe, and by the sign of $\sigma_c$ for the catenation writhe. The parameters $x$, $l$, $\theta$, and $\theta_c$, as well as the sign choice for the plectonemic coiling, are finally determined by free-energy minimization of Eq. (17).

Two features of Eq. (17) lead to a strong coupling of supercoiling and catenation linkages. First, the catenation free-energy cost is strongly increased for small $l_c=(1-x)/(\omega_0|\sigma_c|)$, or for $x\approx 1$. Second, in the final twist term, the extent to which the plectonemic writhe can compensate the internal linkage $\sigma$ is impaired for small $x$. These two trends force $x$ to be determined as a compromise between compressing either the plectonemic or catenation turns. Since the bending and entropic free energies of plectonemic and catenation turns are comparable [16], this compromise should result in comparable values of $l$ and $l_c$.

Results from Eq. (17) are shown in Figs. 3–5. Figure 3(a) shows the free energy as a function of internal double-helix linkage $\sigma$, for fixed catenation of $\sigma_c=0.00$, 0.02, 0.04, 0.06, 0.08, and 0.10. As catenation is added, the free-energy cost of supercoiling at given $\sigma$ increases, due to the crowding of the catenations by the formation of the plectonemic supercoil domains. The minimum of supercoiling free energy shifts from $\sigma=0.00$ for $\sigma_c=0.00$ to roughly $\sigma=0.01$ when $\sigma_c=0.10$. The direction of this shift reflects the fact that the positive writhe of the positive catenations reduces the twist energy in Eq. (17) when $\sigma>0$. Note that the free energy (17) is symmetric under simultaneous sign reversal of $\sigma$ and $\sigma_c$; considering Fig. 3(a), curves for $-\sigma_c$ are therefore obtained by reflection through $\sigma=0$.

In Fig. 4 the supercoil fractions $x$ corresponding to the free energies of Fig. 3(a) are plotted: for large $|\sigma|$, $x$ cannot reach unity for $|\sigma_c|\neq 0$ since the catenation interwinds reduce the amount of molecule available to form plectoneme. For low $|\sigma|$, $x$ is greatly reduced, especially for large $|\sigma_c|$ where the catenations crowd the plectonemic interwinds. An interesting feature of the free energy of Fig. 3(a) is its strong nonconvexity when $\sigma$ and $\sigma_c$ have the same sign. This implies ''phase coexistence'' of tight and loose coiling, and that the free energy requires a Maxwell construction (in Fig. 4 the linear variation of $x$ at small $|\sigma|$ and for $\sigma_c\leqslant 0.02$ is due to phase separation of this type, between tight supercoils and a loosely catenated domain).

Figure 3(b) shows the free energy as a function of catenation $\sigma_c$, for fixed negative supercoiling of $\sigma=0.00$, $-0.02$, $-0.04$, $-0.06$, $-0.08$, and $-0.10$. The $\sigma=0$ curve is the catenation free energy studied in Eq. 21 and Fig. 8 of Ref. [16], and has its minimum at $\sigma_c=0$. For right-handed cat-

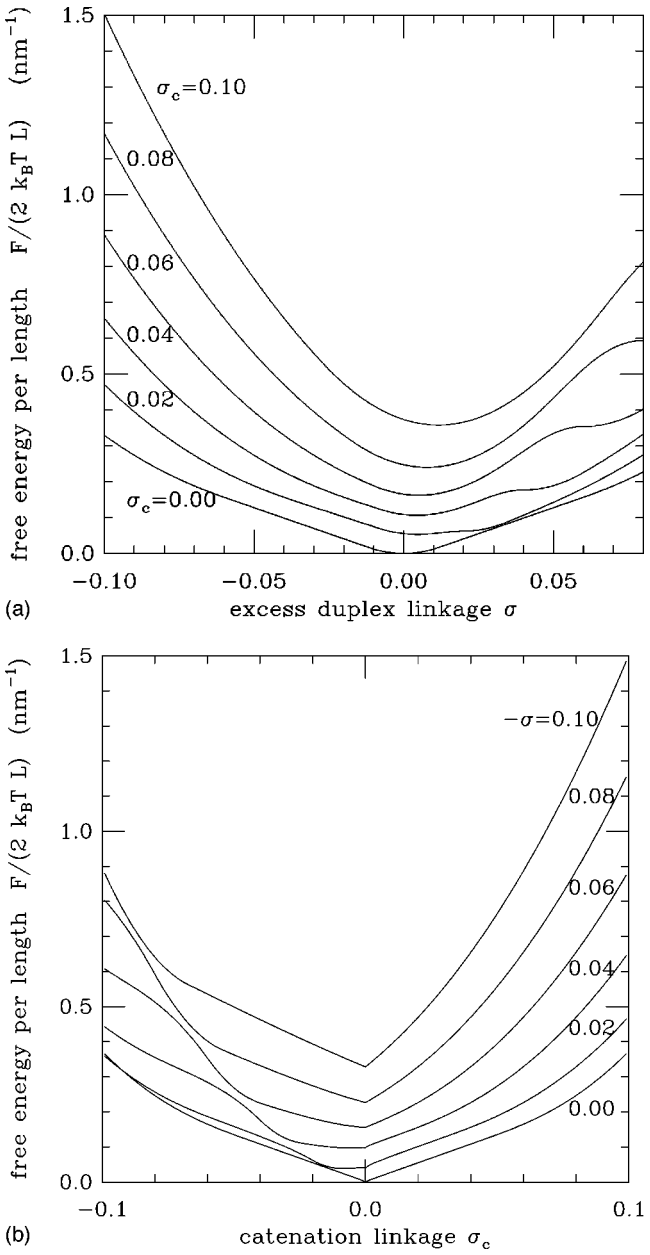


FIG. 3. Free energies of two toroidally catenated DNAs which are also supercoiled, demonstrating the coupling between catenation linkage $\sigma_c$ and internal double helix (supercoiling) linkage $\sigma$. (a) Free energy as a function of $\sigma$ for the cases $\sigma_c=0.00$ (lowest curve), 0.02, 0.04, 0.06, 0.08, and 0.10 (highest curve). The free-energy cost of negative supercoiling ($\sigma<0$) increases with increasing positive catenations between the two chains ($\sigma_c>0$); at the same time, the free-energy minimum shifts to $\sigma>0$. (b) Free energy as a function of $\sigma_c$, for the cases $\sigma=0.00$ (lowest curve), $-0.02$, $-0.04$, $-0.06$, $-0.08$, and $-0.10$ (highest curve). For strong negative supercoiling ($\sigma<-0.05$), crowding of catenations by the supercoils leads to a steepening of the increase of the free energy with either sign of catenation, even at $\sigma_c=0$.

enations ($\sigma_c>0$), addition of negative supercoiling always increases the free-energy cost of catenations. The behavior of the free energy for left-handed catenations ($\sigma_c<0$) is more complicated: for small amounts of negative supercoiling [$\sigma=-0.02$ curve in Fig. 3(b)], the minimum catenation state is shifted away from $\sigma_c=0$. This is the counterpart of the

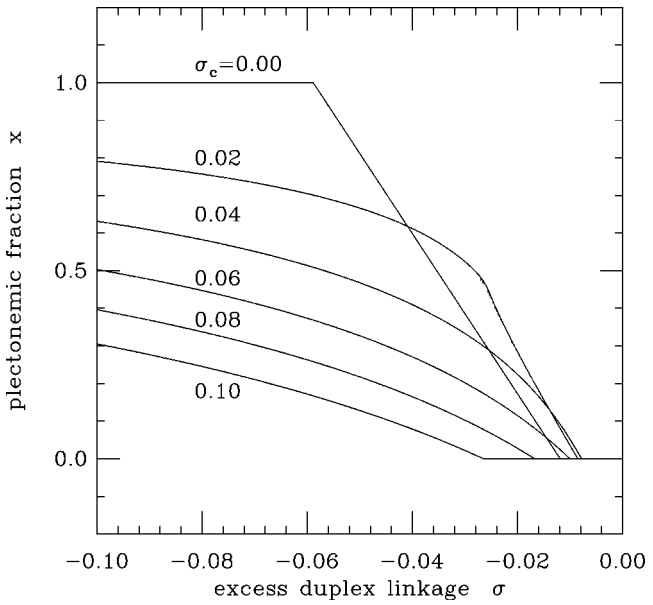


FIG. 4. Supercoil fraction $x$ for catenated, supercoiled molecules as a function of $\sigma$, for $\sigma_c=0.00$, 0.02, 0.04, 0.06, 0.08, and 0.10 [corresponding to the curves of Fig. 3(a)]. For large $|\sigma|$, a high fraction of the molecule is supercoiled, although in the presence of catenation $x<1$ is required. For lower $\sigma$, less of the molecule is supercoiled, an effect which is enhanced by the presence of catenation.

shift in Fig. 3(a) arising from the reduction of twist energy for $\sigma<0$ by the negative writhe of negative catenations. Again, there is nonconvexity in the free energy when $\sigma_c$ and $\sigma$ have the same sign. This will lead to phase separation of the catenation nodes.

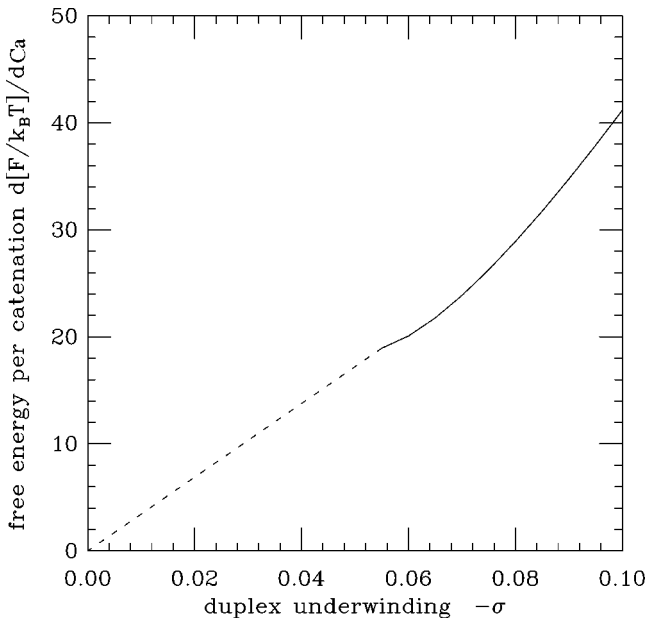


FIG. 5. Free energy per catenation added at zero catenation ($dF/d\mathrm{Ca}[\mathrm{Ca}=0]$) as a function of supercoil linkage $\sigma$. As $\sigma$ is made increasingly negative, there is a progressively higher free-energy cost of each added catenation, even at zero catenation. The solid curve shows the result of Eq. 17, while the dashed curve is a sketch of the expected rapid drop of the free-energy cost to zero (see text).

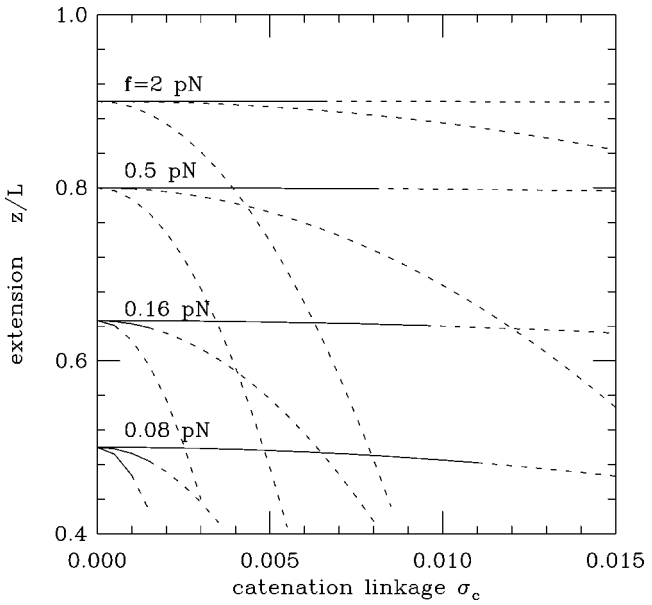


FIG. 6. Extension $z/L$ as a function of catenation linkage $\sigma_c$, for two DNAs subjected to fixed force, according to the model of Sec. III. Supercoiling is unconstrained ($\mu=0$). Each triplet of curves (the curves of each triplet meet at $\sigma_c=0$) shows results for fixed tension and three DNA lengths, $L=1.0$ $\mu$m ($\approx$3 kb, top), $L=16$ $\mu$m ($\approx$50 kb, middle, the size of λ-DNA commonly used in micromanipulation experiments), and $L=\infty$ (bottom). The curves are solid where the interwinding torque $\tau<1$ (the regime where the theory is quantitative, see text) and dashed for $\tau>1$ (where the model has a winding instability, see text). Results are shown for tensions on each DNA of $f=2$ pN (top triplet of curves), 0.5 pN, 0.16 pN, and 0.08 pN (bottom triplet). For increasing $L$ the width of the $f$ vs $\sigma_c$ curves decreases, as the effective twist modulus of the catenated chains contributes progressively less to the elasticity.

For tight supercoiling ($\sigma<-0.04$) the minima of the free-energy curves of Fig. 3(b) are at the ''cusps'' at $\sigma_c=0$, or for decatenated chains. In this regime, catenation crowding by the supercoils is the dominant effect, pushing the free energy up regardless of the sign of $\sigma_c$. This effect, and the cusp at $\sigma_c=0$, follow from the geometrical relation (13) between $1-x$ and $\sigma_c$. For tight coiling, there will be little writhe in the catenation domain ($\theta_c\approx\pi/2$), so the effect of a small number of catenations is simply to reduce the length of the molecule available to form plectonemic supercoils, making the free energy increase as $|\sigma_c|$. There is no corresponding cusp as a function of $\sigma$ in Fig. 3(a) because small amounts of double-helix linkage may be made up by DNA twisting along the entire length of chain, with no need of a supercoiled domain or any writhe at all.

At zero catenation, the free energy is increased as supercoiling is added, and also the free energy per added positive catenation [slopes of the free energy curves of Fig. 3(b) at $\sigma_c=0^+$] increases with tight negative supercoiling ($\sigma<-0.05$). The free energy per added positive catenation, at zero catenation [$dF/d\mathrm{Ca}|_{\mathrm{Ca}=0^+}$; see Eq. (23) of Ref. [16]] is shown in Fig. 5 as a function of $\sigma<0$. This quantity represents the free energy available to direct removal of the last few catenations between two DNAs by topoisomerases [16]. For tight supercoiling ($\sigma<-0.05$, solid line), the free-energy cost of adding just one positive catenation to even nearly decatenated chains is large, starting from roughly $20k_BT$ for $\sigma\approx-0.05$. In this regime the coiling is sufficiently tight to generate a large free energy penalty for insertion of even one positive catenation.

For low levels of supercoiling where $l>A$ ($\sigma<0.01$, see Ref. [5]), and in the limit $\mathrm{Ca}\to0$, the catenation free energy behaves as $F\approx-k_BT\Delta\mathrm{LkCa}/[(L/A)\ln(L/A)]+\mathcal{O}(\mathrm{Ca}^2,\Delta\mathrm{Lk}^2)$ (see Sec. II A) and therefore the free-energy cost of a single catenation will go to zero as $dF/d\mathrm{Ca}\approx-k_BT\omega_0A\sigma/[2\pi\ln(L/A)]$ for small $\sigma$ [this will very slightly shift the catenation free-energy minima of Fig. 3(b) for $|\sigma|<0.01$]. A further complication is that for $|\sigma|<0.05$ the free energy of catenation is not quite convex for $\sigma_c>0$ [see Fig. 3(b); the nonconvexity is barely noticeable compared to that in Fig. 3(a)]. Phase separation of tight and loose coiling is again indicated, and a Maxwell construction is again required to estimate free energy as a function of catenation in this regime (similar effects were previously discussed in Ref. [16]).

Instead of patching together a Maxwell construction with the molecule-length-dependent small-$\sigma_c$ behavior, the low-$\sigma$ free energy per catenation is just sketched with a dashed line in Fig. 5. The precise behavior of the free energy per catenation at zero catenation should first be linear for $\sigma<-0.01$. Note that the range and slope of the linear behavior are $L$-dependent (Sec. II A). The linear behavior will be followed by a regime where there is a gradual increase of the free energy per added catenation with supercoiling, and then finally the free energy per catenation will increase rapidly for $\sigma<-0.05$ when the plectonemic domains start to strongly compress added catenations.

Model (17) is appropriate in the tight coiling regime where the free energy per length exceeds $k_BT/A\approx0.02k_BT/\mathrm{nm}$, or for all of the curves shown in Figs. 3(a) and 3(b) except for the loose-coiling regime near to $\sigma=\sigma_c=0$. For loose coiling, the fluctuation model of Sec. II A applies. Finally, note that the use of single domains (Fig. 2) is a mean-field simplification; for sufficiently long molecules, multiple plectonemic domains will be entropically favored (an analogous effect is the necessity of branch defects on large plectonemic supercoils [5]). However, the fluctuation of domain positions will contribute only $\approx k_BT$ per domain to the free energy. Therefore, accounting for multiple plectonemic domains will only slightly change the free energy for tight coiling, which will be dominated by the competition between DNA elasticity *vs* confinement entropy in Eq. (17).

## III. ELASTICITY OF BRAIDED, SUPERCOILED DNAS

DNA micromanipulation experiments have developed to the point where single molecules may be subjected to controlled stretching forces and twisting torques, so as to constrain their extensions and their linkages [9,10]. One can imagine carrying out such an experiment with *two* molecules, and controlling both intramolecule and intermolecule linkages, with separate molecule twisting and interwinding torques. One way to do this might be to control the twisting of the chains by using a magnetic field to set the direction of the magnetic moment of magnetic beads affixed to the molecule ends, while applying intermolecule winding via ma-

nipulation of the same two beads with twin laser ''tweezers.'' Such an experiment would be able to probe the interaction of catenation and supercoiling, through its influence on the chains' entropic elasticity. This situation is described by the following model:

$$\frac{E}{k_BT}=\int_0^L ds\left\{\frac{A}{2}\left[\left(\frac{d\hat{\mathbf{t}}_1}{ds}\right)^2+\left(\frac{d\hat{\mathbf{t}}_2}{ds}\right)^2\right]-\frac{f\hat{\mathbf{z}}}{k_BT}\cdot(\hat{\mathbf{t}}_1+\hat{\mathbf{t}}_2)\right\}$$
$$-2\pi\tau\mathrm{Ca}-2\pi\mu(\mathrm{Wr}_1+\mathrm{Wr}_2)-\frac{L\mu^2}{C}, \tag{18}$$

where the force $f$ (applied to *each* chain) is coupled to chain extension, while the torque $k_BT\tau$ is coupled to intermolecule winding or catenation.

The Lagrange multiplier $\mu$ is introduced to control the molecule writhes; $k_BT\mu$ is the twisting torque applied to the individual molecules. To see this, consider the model (18) where the final constant term $\propto\mu^2$ is replaced with microscopic molecule twist energies:

$$\frac{C}{2}\int_0^L ds[\Omega_1^2+\Omega_2^2]-2\pi\mu[\Delta\mathrm{Tw}_1+\Delta\mathrm{Tw}_2]. \tag{19}$$

Given that $\Delta\mathrm{Tw}=\int_0^L ds\Omega_i/2\pi$, and that $\Delta\mathrm{Lk}_i=\Delta\mathrm{Tw}+\mathrm{Wr}$, it follows that the twist fluctuations can be integrated out, leaving Eq. (18) including the final constant term, and giving the twist expectation values

$$\langle\Delta\mathrm{Tw}_i\rangle=\frac{\mu L}{2\pi C}. \tag{20}$$

Therefore, Eq. (18) describes the conformations of molecules with $\mu$ coupled to molecule excess linkages, i.e., $\mu$ is a twisting torque applied to each molecule. For given $\mu$, the excess linkages can be computed by adding the writhe expectations of Eq. (18) to the twist expectations (20).

The model (18) requires computer simulation for its general study. However, in the limit of large $f\gg k_BT/A$, the chains will be nearly straight with small transverse fluctuations. It is therefore possible to study the small transverse fluctuations of the chain tangents:

$$\mathbf{t}_{\perp,i}=\hat{\mathbf{t}}_i-(\hat{\mathbf{z}}\cdot\hat{\mathbf{t}}_i)\hat{\mathbf{z}}. \tag{21}$$

The two chain contours to lowest order in the transverse fluctuations are

$$\mathbf{r}_i(s)=\mathbf{r}_i(0)+s\hat{\mathbf{z}}+\int_0^s ds'\mathbf{t}_{\perp,i}(s')+\mathcal{O}(\mathbf{t}_{\perp,i}^2). \tag{22}$$

To express Eq. (18) in terms of these small fluctuations, $\mathrm{Wr}_i$ and Ca must be expanded in $\mathbf{t}_{\perp,i}$. The writhes may be expressed as [5,13,14,28]

$$\mathrm{Wr}_i=\frac{1}{4\pi}\int_0^L ds\hat{\mathbf{z}}\cdot\mathbf{t}_{\perp,i}\times\frac{d\mathbf{t}_{\perp,i}}{ds}+\mathcal{O}(\mathbf{t}_{\perp,i}^3). \tag{23}$$

To see what to do with Ca, first note that for sufficiently weak torques, the transverse distance between corresponding points along them grows as $\langle\{[\mathbf{r}_1(s)-\mathbf{r}_2(s)]\times\hat{\mathbf{z}}\}^2\rangle\approx k_BTs/f$ [30]. The longitudinal fluctuation of corresponding chain positions is much smaller, $\langle\{\hat{\mathbf{z}}\cdot[\mathbf{r}_1(s)-\mathbf{r}_2(s)]\}^2\rangle-\langle\hat{\mathbf{z}}\cdot[\mathbf{r}_1(s)-\mathbf{r}_2(s)]\rangle^2\approx(s/A^{1/2})(k_BT/f)^{3/2}$. So, the difference variable $\mathbf{u}(s)\equiv[\mathbf{r}_1(s)-\mathbf{r}_2(s)]/2$, as well as fluctuations of the mean tangent vector $\mathbf{t}(s)\equiv[\mathbf{t}_1(s)+\mathbf{t}_2(s)]/2$, both become perpendicular to $\hat{\mathbf{z}}$ as $f\to\infty$. Corresponding points along the two chains are essentially in registry for large forces.

This suggests decomposition of the catenation of two double helicies into ''twist'' of $\hat{\mathbf{u}}$ and ''writhe'' of the centerline of the two chains, $\mathbf{r}\equiv[\mathbf{r}_1+\mathbf{r}_2]/2$, in the same manner as was done for linkage of the two nucleotide chains in one double helix:

$$\mathrm{Ca}\approx\mathrm{Wr}[\mathbf{r}(s)]+\frac{1}{2\pi}\int ds\hat{\mathbf{u}}\times\frac{d\hat{\mathbf{u}}}{ds}\cdot\frac{d\mathbf{r}}{ds}\left|\frac{d\mathbf{r}}{ds}\right|^{-1}. \tag{24}$$

The final ''twist'' term counts the circulation of $\hat{\mathbf{u}}$ around the centerline of the two chains. Equation (24) is asymptotically exact for $|\mathbf{u}|$ much smaller than the typical distance over which $\hat{\mathbf{t}}$ reorients, and it is therefore reasonable for highly extended chains.

Plugging these results together allows Eq. (18) to be evaluated to quadratic order in $\mathbf{t}_{\perp,i}$,

$$\frac{E}{k_BT}=\int_0^L ds\left\{A\left(\frac{d\mathbf{t}_\perp}{ds}\right)^2+\frac{f}{k_BT}\mathbf{t}_\perp^2-\left(\frac{\tau}{2}+\mu\right)\hat{\mathbf{z}}\cdot\mathbf{t}_\perp\times\frac{d\mathbf{t}\perp}{ds}+A\left(\frac{d^2\mathbf{u}_\perp}{ds^2}\right)^2\right.$$
$$\left.+\frac{f}{k_BT}\left(\frac{d\mathbf{u}_\perp}{ds}\right)^2-\mu\hat{\mathbf{z}}\cdot\frac{d\mathbf{u}_\perp}{ds}\times\frac{d^2\mathbf{u}_\perp}{ds^2}-\tau\hat{\mathbf{z}}\cdot\hat{\mathbf{u}}_\perp\times\frac{d\hat{\mathbf{u}}_\perp}{ds}\right\}-\frac{2Lf}{k_BT}-\frac{L\mu^2}{C}, \tag{25}$$

where $\mathbf{t}_\perp(s)=[\mathbf{t}_{\perp,1}(s)+\mathbf{t}_{\perp,2}(s)]/2$ and $d\mathbf{u}_\perp(s)/ds=[\mathbf{t}_{\perp,1}(s)-\mathbf{t}_{\perp,2}(s)]/2$. Harmonic fluctuations of the centerline ($\mathbf{t}$) and displacement ($\mathbf{u}$) are decoupled.

The centerline fluctuations may be immediately integrated by the methods of Ref. [26]; on the other hand, the displacement energy has a bunch of simple Gaussian terms, but also has a twist term which depends on $\hat{\mathbf{u}}_\perp$. Here, this final term will be treated in a crude mean-field way, by its replacement with $-\tau[\hat{\mathbf{z}}\cdot\mathbf{u}\times d\mathbf{u}/ds]/\langle u^2\rangle$. This only makes sense when $\langle u^2\rangle\approx k_BTs/f$ does not increase appreciably over a correlation length for the fluctuations $\approx(k_BTA/f)^{1/2}$. Also, hard-core interactions [not explicitly written down in Eq. (25)], which keep $u\geq u_0$ ($u_0\approx 3$ nm), are necessary to make this approximation reasonable [33].

Once the mean-field approximation is made, the free energy follows as

$$\ln Z=\frac{2Lf}{k_BT}+\frac{L\mu^2}{C}-L\int\frac{dq}{2\pi}\left\{\ln\left[Aq^2+\frac{f}{k_BT}+\left(\frac{\tau}{2}+\mu\right)q\right]+\ln\left[Aq^2+\frac{f}{k_BT}+\mu q-\frac{\tau}{\langle u^2\rangle q}\right]\right\}. \tag{26}$$

The integrations are over positive and negative wave numbers. The conditions for the torques to be small perturbations on the free energy are, first, that for the smallest wave numbers the supercoiling torque terms are small, or $\mu<\sqrt{Af/k_BT}$. The same condition should hold for the interwinding torque, but more stringent, the $1/q$ term should not introduce a singularity into the free energy, or $|\tau|<\langle u^2\rangle q_{\min}f/k_BT$. Since $q_{\min}\approx 1/L$ and $\langle u^2\rangle\approx k_BTL/f$, this second condition is $|\tau|<1$. Beyond this scale of torque the mean-field energy (26) displays a winding instability [34].

Expansion to second order in the torques gives

$$\ln Z=\frac{L}{A}\left\{\frac{2Af}{k_BT}+\frac{A\mu^2}{C}-\left(\frac{4fA}{k_BTA}\right)^{1/2}+\frac{1}{4}\left(\frac{k_BT}{4Af}\right)^{1/2}[(\tau/2+\mu)^2+\mu^2]\right\}$$
$$+\frac{LA^3}{4\pi\langle u^2\rangle^2}\left(\frac{k_BT}{Af}\right)^{5/2}\int\frac{dx}{x^2(1+x^2)^2}\tau^2-\frac{LA}{2\pi\langle u^2\rangle}\left(\frac{k_BT}{Af}\right)^{3/2}\int\frac{dx}{(1+x^2)^2}\mu\tau. \tag{27}$$

In the final two terms, the integration variable is $x=(k_BTA/f)^{1/2}q$.

The computation of the final two terms of Eq. (27) has not yet accounted for the growth of mean-squared chain displacement with contour length, $\langle u(s)^2\rangle\approx k_BTs/f$. The integrals in Eq. (27) can be used to account for subsections of the chain over which $\langle u^2\rangle$ varies slowly compared to the tangent correlation length $(k_BTA/f)^{1/2}$. Contributions of chain subsections $L/2^{n+1}<s<L/2^n$ may be computed (by replacing $L\to L/2^n$ for each subsection, including in the long-wavelength cutoff needed to make the $\propto\tau^2$ integral finite) and added up. This summation ends at a short-distance cutoff scale $\xi_0=u_0^2f/k_BT$, where the two chains come into contact (for large $f$ the consistency requirement for the mean-field approximation, $d\langle u^2\rangle/ds<u^2/[k_BTA/f]^{1/2}$, holds for $s>\xi_0$). The last two terms of Eq. (27) add up to

$$\left[k_1\tau^2-k_2\left(\frac{k_BT}{Af}\right)^{1/2}\mu\tau\right]\ln\frac{k_BTL}{u_0^2f}, \tag{28}$$

where $k_1$ and $k_2$ are $\mathcal{O}(1)$ constants.

This summation scheme accounts for the growth of $\langle u^2\rangle$ and leads to a $\ln L$-dependent interwinding elasticity (reminiscent of the weak-interwinding elasticity of unstretched chains of Sec. II [32]), and supercoiling-interwinding interaction. For $L\to\infty$, these logarithms are small compared to the extensive $\tau^2$ and $\tau\mu$ terms, and interwinding elasticity of stretched DNAs thus becomes almost entirely due to the writhing fluctuations (this is in contrast to the elasticity of a twisted double helix where elastic twist and writhing contributions both contribute even for $L\to\infty$ [13,16]). However, for finite-$L$ DNAs under finite forces, the $\sim\tau^2\ln L$ twist contribution can be comparable to the $\sim\tau^2f^{-1/2}L$ writhing term, and therefore should be kept for comparison to experiments and simulations. On the other hand, the $\sim\mu\tau f^{-1/2}\ln L$ term is always small compared to the corresponding extensive term $\sim\mu\tau f^{-1/2}L$ and may be ignored.

The elasticity of the chains follows from the free energy via $\langle z\rangle=(1/2)\partial k_BT\ln Z/\partial f$:

$$\left\langle\frac{z}{L}\right\rangle=1-\left(\frac{k_BT}{4Af}\right)^{1/2}-\frac{(\tau/2+\mu)^2+\mu^2}{4}\left(\frac{k_BT}{4Af}\right)^{3/2}-k_1\tau^2\frac{k_BT}{Lf}. \tag{29}$$

For $\tau=\mu=0$, the large-force WLC elasticity is recovered. For general $\mu$ and $\tau$, there is a linear coupling of the supercoiling and interwinding torques. Equation (29) shows that any combination of twisting and interwinding torques always reduces the extension in the high-force limit, relative to free DNA $(\mu=\tau=0)$.

The results can be written in terms of Ca and $\Delta$Lk using their expectation values, $\langle\mathrm{Wr}_i\rangle=\partial\ln Z/\partial(4\pi\mu)$ and $\langle\mathrm{Ca}\rangle=\partial\ln Z/\partial(2\pi\tau)$, and $\Delta\mathrm{Lk}_i=\mu L/(2\pi C)+\langle\mathrm{Wr}_i\rangle$. The linkage of either chain in terms of $\sigma=\Delta\mathrm{Lk}/\mathrm{Lk}_0$ is

$$C\omega_0\sigma=\mu+\frac{C}{8A}\left(\frac{k_BT}{4Af}\right)^{1/2}(\tau+4\mu). \tag{30}$$

The mutual linkage of the two chains in terms of $\sigma_c=\mathrm{Ca}/\mathrm{Lk}_0$ works out to be

$$A\omega_0\sigma_c=2\frac{k_1A}{L}\tau\ln\frac{k_BTL}{u_0^2f}+\frac{1}{8}\left(\frac{k_BT}{4Af}\right)^{1/2}(\tau+2\mu). \tag{31}$$

Figure 6 shows results for the case where supercoiling is unconstrained ($\mu=0$), for extension as a function of catenation at fixed force, taking $k_1=4$ in Eqs. (29), (30), and (31). This type of experiment is the most likely case to be first studied; in fact, preliminary results have been published for two 48 kb DNAs wrapped around one another, by Strick *et al.* [10], and the results of Fig. 6 for two 50 kb chains each under a tension of 2 pN agree reasonably well with Fig. 7A of Ref. [10] for $|\sigma_c|<0.01$. The results for two 3 kb chains held under tensions of 0.08 pN and 0.16 pN also match preliminary Monte Carlo results for the elasticity of catenated chains [29]. There is a strong finite-size effect for $L\approx 10$ kb due to the logarithmic effective twisting elasticity of the two DNAs.

Returning to the case where there is both supercoiling and catenation, one can demonstrate the coupling of $\sigma$ to $\sigma_c$ in $\langle z/L\rangle$ for the $L=\infty$ case where the arithmetic is simplified by

removal of the logarithmic terms. The torque equations (30) and (31) may be then easily inverted:

$$\frac{\tau}{2}+\mu=4A\omega_0\sigma_c\left(\frac{4Af}{k_BT}\right)^{1/2},$$
$$\mu=\frac{C\omega_0(\sigma-\sigma_c)}{1+(C/4A)(4Af/k_BT)^{1/2}}. \tag{32}$$

Eliminating the torques from the extension gives

$$\frac{z}{L}=1-\left(\frac{k_BT}{4A_{\rm eff}f}\right)^{1/2}-\frac{1}{4}(C\omega_0)^2(\sigma-\sigma_c)^2\left(\frac{k_BT}{4Af}\right)^{3/2}+\mathcal{O}(f^{-5/2}), \tag{33}$$

where $A_{\rm eff}=A/[1+4(A\omega_0\sigma_c)^2]$. For $L\to\infty$, fixed nonzero $\sigma_c$ reduces the apparent persistence length; there is no force scale at which this effect vanishes. Any combination of nonzero fixed linkages always reduces the extension, but the reduction effect of fixed $\sigma_c$ can be partially compensated for with $\sigma$ of the same sign (or alternately, extension can be further reduced by addition of $\sigma$ of opposite sign to $\sigma_c$). This follows from a coupling of $\sigma$ to $\sigma_c$ in the free energy of the same sense as that discussed in Sec. II, i.e., an increase in catenation free energy when supercoiling is added with opposite sense to the interwinds. The fixed-linkage free energy can be computed by Legendre transformation of Eq. (27):

$$\frac{F(\sigma,\sigma_c)}{k_BT}=-\ln Z+\mu\frac{\partial\ln Z}{\partial\mu}+\tau\frac{\partial\ln Z}{\partial\tau}=2L\left\{\left(\frac{f}{k_BTA_{\rm eff}}\right)^{1/2}-\frac{f}{k_BT}+\frac{1}{2}\left[1-\frac{C}{4A}\left(\frac{k_BT}{4Af}\right)^{1/2}\right]\times C\omega_0(\sigma-\sigma_c)^2\right\}. \tag{34}$$

The $\sigma$- and $\sigma_c$-dependent terms of this free energy represent the work done during addition of catenation and supercoiling to two chains held at fixed tension $f$.

Finally, it should be noted that the result (33) with $\sigma_c=0$ does not represent the case of elasticity of independent supercoiled chains [13,26], which is instead obtained by setting $\tau=0$ and elimination of the induced catenation

$$\langle\sigma_c\rangle=\frac{\mu}{4A\omega_0}\left(\frac{k_BT}{4Af}\right)^{1/2}\approx\frac{C}{4A}\left(\frac{k_BT}{4Af}\right)^{1/2}\sigma \tag{35}$$

giving an elasticity of the form of Eq. (33) with $\sigma_c=0$, but with the $f^{-3/2}$ term doubled. The alternate case of interwound but torsionally unconstrained chains obtained by setting $\mu=0$ works out to be the first two terms of Eq. (33) with no $f^{-3/2}$ term, thanks to induced supercoiling $\langle\sigma\rangle=\sigma_c$. This induced supercoiling is entirely made up by writhe since the chains are not subject to twist constraint. Note that for $|A\omega_0\sigma_c|\ll1$ the elasticity returns to that of the unconstrained WLC, as noted previously [16].

## IV. HOW DO CELLS SEGREGATE DNAS FOLLOWING THEIR REPLICATION?

All cells are capable of resolving the entanglements between large chromosomal DNAs. This is remarkable, given that the molecules being disentangled exceed the dimensions of the cells by orders of magnitude. In the 1-$\mu$m-long bacterium E. coli, the 4.7 mega-base-pair (Mb) chromosome contains 1.5 mm of DNA. The chromosomal DNA must be replicated in order for E. coli to divide, and it is known that DNA replication is ''semi-conservative,'' meaning that the two single strands of the parental DNA are used as templates to synthesize new strands for each of the child DNAs, and therefore must be unwound. An important question is how E. coli is able to segregate the two copies of its chromosome to the two new cells. Since DNA replication is likely to leave many catenations between the two chromosome copies [22], E. coli must possess an efficient mechanism to convert nonlocal topological entanglements into a force which drives type-II topoisomerases to remove those entanglements.

### A. Negative supercoiling-driven removal of positive catenations

The coupling of catenation to supercoiling discussed above (Sec. II) suggests a mechanism to drive disentanglement of E. coli chromosomes [16]. Since negative supercoiling leads to an increase in the free-energy cost of positive catenations, steady addition of negative supercoiling (by gyrase, an ATP-powered enzyme which takes links out of double-helix DNA [22]) will make any number of positive catenations progressively more thermodynamically unfavorable. At fixed Ca, in order to strike a balance between the density of supercoil and catenation interwinding, the catenations will become increasingly crowded together, and will cost an increasing amount of free energy, as supercoiling is added. For low amounts of supercoiling, the effects of the catenation free-energy minimum being at $\sigma_c\neq0$, and tight-loose catenation phase coexistence [both present in the model of Sec. II B for $-\sigma<0.05$, see Fig. 4(b)] will interfere with this mechanism.

Once crowding is established, if there is a type-II topoisomerase capable of passing double helix through double helix, but otherwise without any special bias to its function, it will be directed by the free energy of Sec. II to remove the catenations. As supercoiling is made more negative (by continual action of gyrase), the free energy per positive catenation will be increased. This will lead to a much higher probability for positive catenations to be removed (or ''resolved'') by the unbiased type-II topoisomerase than for additional positive catenations to be accidentally added. Thus negative supercoiling introduced by gyrase will ''squeeze'' out the positive catenations likely remaining after DNA replication in the presence of a ''double-strand-passing'' type-II topoisomerase. Finally, when all the catenations are removed, the two DNAs will tend not to reentangle because they will be tightly negatively supercoiled [18].

It is likely that not only toroidal catenations can be removed by this scheme, but also that more general entanglements—knots on a single circular DNA, and general linkages between two or more DNAs—can be made thermodynamically unfavorable if the individual DNAs are supercoiled. This needs to be studied via computer simula-

tion, or via scaling calculations similar to those of Sec. II C.

One might object to this proposed mechanism on the grounds that the unbiased double-strand-passing topoisomerase could take out the supercoiling as well as the catenation (the local shape of DNA in negative plectonemic supercoils is similar to that in positive catenanes [22]). However, as long as the supercoiling is replenished by gyrase at a greater rate than it can be removed by the double-strand-passing topoisomerase (or other supercoil-relaxing topoisomerases such as topo I), the supercoiling will increase, and the catenation will consequently decrease. Thus this mechanism also suggests that the net activity (determined by both concentration and intrinsic processivity of each unit) of the unbiased double-strand-passing enzyme should not be too great.

There is a likely suspect for this proposed ''unbiased type-II topoisomerase'' [22]: in E. coli it is called topoisomerase IV. Topo IV is homologous in structure and similar in function to the type-II topoisomerase from eukaryote cells. Each double strand passage appears to require roughly 2 ATP hydrolysis events, which release roughly $20k_BT$ of stored chemical energy. However, this energy is not transferred to supercoiling: topo IV has no intrinsic ability to supercoil double-stranded circular DNA.

### B. Experiments *in vivo* and *in vitro* show decatenation by topo IV to be enhanced by supercoiling

Recent experiments have established that gyrase increases the efficiency of decatenation by topo IV of even small circular ''plasmid'' DNAs *in vitro* and *in vivo*, and suggest a role for gyrase in the final stages of decatenation [24]. For example, a test-tube study of 3 kb + 4 kb catenanes showed decatenation by topo IV to be roughly four times faster when the plasmids were supercoiled than when they were unsupercoiled (Fig. 2 of Ref. [24]). In a different study of catenated 2.9 kb and 0.6 kb circles in E. Coli, a strong enhancement of decatenation by supercoiling was reported (Fig. 6 of Ref. [25]). Finally, genetic experiments indicate that cells with defective gyrase have an inability to disentangle replicated DNAs [35–37], and also contain circular DNAs which are highly knotted [38].

The supercoiling-driven decatenation scheme described above simply explains these observations. Additional observations of rather less efficient decatenation in the absence of topo IV may also be interpreted in this way given the reasonable assumption that gyrase itself has some weak ability to pass double strands [23]. Further *in vivo* and *in vitro* experiments on longer DNAs are indicated to try to understand whether supercoiling-driven disentanglement works in the test tube, and is in fact a mechanism used in eubacteria.

The $-\sigma \approx 0.05$ threshold for the supercoil crowding of catenations to guarantee a strong driving force toward the decatenated state indicates that the crowding-decatenation mechanism described above should work reliably only for $-\sigma > 0.05$. This is in accord with the observation that native circular prokaryote DNAs are roughly 5% underwound (if pulled out to be linear, they would have an 11 bp helix repeat instead of the 10.5 bp repeat of relaxed DNA). Perhaps the advantage of keeping DNAs disentangled from one another is a reason why eubacteria (and halophilic archaebacteria [39]) have enzymes which keep their circular DNAs tightly negatively supercoiled.

The notable exceptions to this ''negative supercoiling rule'' of bacteria are the extremely thermophilic archaebacteria which live under high pressures, and at temperatures of up to 100 C [39]. These bacteria have positively supercoiled circular chromosomes and plasmids, driven by the ''reverse gyrase'' enzyme. Currently it is thought that the positive supercoiling is present mainly to prevent thermal denaturation and breakdown of the DNA. Little is known about the details of chromosome and plasmid segregation in these species.

Finally, note that in eukaryotes (cells with nuclei: fungi, plants, animals) it is currently thought that there is no gyrase and no plectonemic supercoiling. However, an analogous crowding-resolution scheme has been proposed for eukaryote cells [40]. Instead of supercoiling, this scheme is based on attachment of chromosomes to themselves to form ''loop'' domains which, when crowded together, generate osmotic pressure via excluded volume effects, which in turn drives entanglement resolution.

### C. ''Maxwell demon'' properties of topo IV

A remarkable feature shared by E. coli topo IV and eukaryote topo II was revealed by Rybenkov *et al.*, *in vitro* on 5–10 kb knot, supercoil, and catenane substrates [41]. These enzymes were shown to be able to resolve topological entanglements down to levels $\approx 0.01$ times that obtained in thermal equilibrium for phantomlike chains. Although this is reminiscent of the ''Maxwell demon,'' these enzymes release stored energy from ATP as they act, so there is no violation of the second law of thermodynamics. However, exactly how these enzymes use stored energy to make the decisions necessary to simplify the topology of large polymers below that expected in thermal equilibrium remains to be understood.

Perhaps the knot-resolving capability can be explained by the hypothesis that topo IV and topo II can bind and resolve the triple crossing of trefoil knots, which are the most common self-entanglement for DNAs of $\leqslant 10$ kb in length. It is also to be noted that for the lengths of chains studied, the equilibrium probability that the chains were unknotted was roughly 2% [41]. Therefore knots and other entanglements are not small perturbations on $\approx 10$ kb DNAs; for the molecules studied by Rybenkov *et al.* [41], introducing a knot costs free energy $\approx -k_BT \ln(0.02) \approx 4k_BT$. Therefore strong conformational changes should be introduced by knots on 10 kb plasmids, which might be recognized by topo IV (or topo II), and then preferentially resolved using the energy from ATP hydrolysis.

Any mechanism to explain this behavior must be local (since topo IV and topo II are $<10$ nm in size), and therefore will become much less effective for longer chains. For example, a repeat of the experiment of Rybenkov *et al.* [41] with chains long enough to be 50% knotted by thermal fluctuations should display a smaller difference between thermal and topo IV (or topo II) knotting levels. For long DNAs in the crowded confines of a cell, robust entanglement-localization mechanisms such as the supercoil-crowding

mechanism proposed above are needed to guarantee entanglement resolution.

It is to be stressed that there is no conflict between the ''Maxwell demon'' behavior of topo IV/topo II and the results of this paper, which indicate that entanglements can be made more costly in free energy by introduction of supercoiling. The experimental fact that topo IV removes entanglements more quickly from supercoiled than from unsupercoiled substrates supports the supercoil-crowding idea proposed above [24,25]. This mechanism will of course be enhanced by topo IV's ability to reduce entanglement complexity below that expected in thermal equilibrium [41]. Supercoil crowding of entanglements and topo IV's ''demonic'' knot-recognizing abilities should be thought of as complementary features of the entanglement removal system of E. coli.

## ACKNOWLEDGMENTS

The author thanks J.-F. Allemand, D. Bensimon, N. Cozzarelli, V. Croquette, N. P. Higgins, T. Imbo, S. Leibler, D. R. Nelson, M. D. Schmidt, T. Strick, E. D. Siggia, N. Trun, and A. V. Vologodskii for helpful discussions. Acknowledgment is made to the Donors of the Petroleum Research Fund, administered by the American Chemical Society, for partial support of this research. This work was also partially supported by the Research Corporation.

[1] P. G. de Gennes, *Scaling Concepts in Polymer Physics* (Cornell University Press, Ithaca, NY, 1983), Chap. 1.

[2] M. D. Frank-Kamenetskii and A. V. Vologodskii, Usp. Fiz. Nauk **134**, 641 (1981).

[3] N. R. Cozzarelli, T. C. Boles, and J. White, in *DNA Topology and its Biological Effects*, edited by N. R. Cozzarelli and J. C. Wang (Cold Spring Harbor Laboratory, Cold Spring Harbor, NY, 1990), Chap. 4.

[4] G. N. Giaever, L. Snyder, and J. C. Wang, Biophys. Chem. **29**, 7 (1988); K. Drlica, Mol. Microbiol. **6**, 425 (1992).

[5] J. F. Marko and E. D. Siggia, Science **265**, 506 (1994); Phys. Rev. E **52**, 2912 (1995).

[6] R. E. Deprew and J. C. Wang, Proc. Natl. Acad. Sci. USA **11**, 4279 (1975); D. E. Pulleyblank, M. Shure, D. Tang, J. Vinograd, and H.-P. Vosberg, *ibid.* **11**, 4280 (1975).

[7] A. V. Vologodskii and N. R. Cozzarelli, Annu. Rev. Biophys. Biomol. Struct. **23**, 609 (1994).

[8] T. C. Boles, J. H. White, and N. R. Cozzarelli, J. Mol. Biol. **213**, 931 (1990).

[9] T. R. Strick, J.-F. Allemand, D. Bensimon, A. Bensimon, and V. Croquette, Science **271**, 1835 (1996).

[10] T. R. Strick, J.-F. Allemand, D. Bensimon, A. Bensimon, and V. Croquette, Biophys. J. **74**, 2016 (1998).

[11] K. V. Klenin, A. V. Vologodskii, V. V. Anshelevich, A. M. Dykhne, and M. D. Frank-Kamenetskii, J. Mol. Biol. **217**, 413 (1991); A. V. Vologodskii, S. D. Levene, K. V. Klenin, M. D. Frank-Kamenetskii, and N. R. Cozzarelli, *ibid.* **227**, 1224 (1992).

[12] A. V. Vologodskii and J. F. Marko, Biophys. J. **73**, 123 (1997).

[13] J. D. Moroz and P. Nelson, Proc. Natl. Acad. Sci. USA **94**, 14 418 (1997); Macromolecules **31**, 6333 (1998).

[14] C. Bouchiat and M. Mezard, Phys. Rev. Lett. **80**, 1556 (1998).

[15] J. D. Moroz and R. D. Kamien, Nucl. Phys. B **506**, 695 (1997).

[16] J. F. Marko, Phys. Rev. E **55**, 1758 (1997).

[17] J. Wang and H. Schwartz, J. Mol. Biol. **15**, 111 (1967).

[18] V. V. Rybenkov, A. V. Vologodskii, and N. R. Cozzarelli, J. Mol. Biol. **267**, 312 (1997).

[19] S. D. Levene, C. Donahue, T. C. Boles, and N. R. Cozzarelli, Biophys. J. **69**, 1036 (1995).

[20] O. Sundin and A. Varshavsky, Cell **21**, 103 (1980).

[21] D. E. Adams, E. M. Shektman, E. L. Zechiedrich, M. B. Schmid, and N. R. Cozzarelli, Cell **71**, 277 (1992).

[22] C. J. Ullsperger, A. V. Vologodskii, and N. R. Cozzarelli, *Nucleic Acids and Molecular Biology*, edited by F. Eckstein and D. M. J. Lilley (Springer-Verlag, Berlin 1995), Vol. 9, pp. 115–142.

[23] E. L. Zechiedrich and N. R. Cozzarelli, Genes Dev. **9**, 2859 (1995).

[24] C. Ullsperger and N. R. Cozzarelli, J. Biol. Chem. **49**, 31 549 (1996).

[25] E. L. Zechiedrich, A. B. Khodursky, and N. R. Cozzarelli, Genes Dev. **11**, 2580 (1997).

[26] J. F. Marko, Phys. Rev. E **57**, 2134 (1998).

[27] See D. M. Crothers, J. Drak, J. D. Kahn, and S. D. Levene, Methods Enzymol. **212**, 3 (1992) for evidence for $C \approx 75$ nm. See also Ref. [13] for a discussion of the possibility of a large ''bare'' value of $C \approx 110$ nm, and also D. Bensimon, D. Dohmi, and M. Mezard, Europhys. Lett. **42**, 97 (1998); P. Nelson, Phys. Rev. Lett. **80**, 5810 (1998) for a discussion of the possibility of a large bare bending constant $A \approx 60$ nm. These papers argue that the observed smaller $C$ and $A$ come about as a result of thermal fluctuations and quenched disorder, respectively.

[28] J. H. White, Am. J. Math. **91**, 693 (1969); F. B. Fuller, Proc. Natl. Acad. Sci. USA **68**, 815 (1971).

[29] J. F. Marko and A. V. Vologodskii (unpublished).

[30] J. F. Marko and E. D. Siggia, Macromolecules **28**, 8759 (1995).

[31] S. Prager and H. L. Frisch, J. Chem. Phys. **46**, 1475 (1967); S. F. Edwards, Proc. Phys. Soc. London **91**, 513 (1967); S. F. Edwards and J. W. Kerr, J. Phys. C **5**, 2289 (1972); N. Saitoh and Y.-D. Chen, J. Chem. Phys. **59**, 3701 (1973).

[32] J. Rudnick and Y. Hu, Phys. Rev. Lett. **60**, 712 (1988); for analogous exact results in two dimensions, see B. Duplantier and H. Saleur, *ibid.* **60**, 2343 (1988).

[33] The fluctuations of Eq. (30) can be treated in more detail using polar $u_\perp$ coordinates, and using an additional Gaussian field to allow the bending energy to be treated using Schrödinger-equation-like transfer-matrix techniques.

[34] Note that tight-loose braid phase separation, a type of winding instability, has been predicted for braids under *zero* tension for a torque $\tau \approx 1$, see Ref. [16].

[35] E. Orr, N. F. Fairweather, I. B. Holland, and R. H. Pritchard, Mol. Gen. Genet. **177**, 103 (1979).

[36] T. R. Steck and K. Drlica, Cell **36**, 1081 (1984).
[37] T. Ogura, H. Niki, M. Morita, M. Hasegawa, C. Ichinose, and S. Hiraga, J. Bacteriol. **172**, 1562 (1990).
[38] K. Shishido, N. Komiyama, and S. Ikawa, J. Mol. Biol. **195**, 215 (1987).
[39] P. Forterre, F. Charbonnier, E. Marguet, F. Harper, and G. Henckes, Biochem. Soc. Symp. **58**, 99 (1992).
[40] J. F. Marko and E. D. Siggia, Mol. Cell Biol. **8**, 2217 (1998).
[41] V. V. Rybenkov, C. Ullsperger, A. V. Vologodskii, and N. R. Cozzarelli, Science **277**, 690 (1997).